Development of an Inertial Measurement System for the Kinematic Analysis of Human Gait*

Angel Camacho[1], Pedro Garcia-Enriquez[1], Manuela Gomez-Correa[2], Mauricio Gonzalez-Palacio[3], Diana Tobon-Vallejo[4], David Cruz-Ortiz[1], Mariana Ballesteros[2]

***Abstract*—The analysis of gait is a field of study whose popularity has grown due to its broad range of applications. Consequently, the development of tools for capturing gait has also seen a significant increase. This article presents the development of a system for gait analysis named STEPIO, which consists of four portable wireless modules, each equipped with a board comprised of a microcontroller and an inertial sensor. The system includes an intuitive graphical user interface that allows the acquisition, visualization, processing, and storage of the signals. The system offers a low-cost solution and the possibility of conducting studies in different environments and implementing innovative tools like the Internet of Things. To evaluate the performance of the system, 15 subjects without any diagnosed neuromusculoskeletal pathologies participated in the experimental protocol in which the range of motion of the knee and hip articulations was measured and compared with a reference optical system, resulting in a root mean square error of 2.7 degrees and a mean deviation of 2.44 degrees.**

***Index Terms*—Inertial Measurement System, Kinematic Analysis, Gait cycle, Internet of Things.**

I. Introduction

The gait cycle is defined as the alternating and rhythmic movements of the lower limbs that facilitate human locomotion. When a person learns to walk, the gait cycle evolves to optimize movement, minimizing physical effort and energy expenditure [1]. The study of human gait has become increasingly important because various gait parameters provide valuable insights into an individual's cognitive and physical state [2]. Consequently, gait analysis is essential for assessing locomotor function and physical performance, with medical applications for diagnosing, treating, and monitoring movement disorders. It also supports the development of new rehabilitation techniques, medical device design, and assistive technologies, being useful in the validation of active prostheses [3].

*This work was supported in part by the Instituto Politécnico Nacional, under Grants: SIP-20250223 and SIP-20250253. D. Cruz-Ortiz and M. Ballesteros thanks the support provided by Secretaría de Educación, Ciencia, Tecnología e Innovación de la Ciudad de México (SECTEI) under the grant SECTEI/081/2024.

[1]Medical Robotics and Biosignals Lab, UPIBI-Instituto Politécnico Nacional, Av. Acueducto S/N, La Laguna Ticoman, Gustavo A. Madero, 07340, Mexico City, Mexico. email: acamacho11700@alumno.ipn.mx, pgarciae1700@alumno.ipn.mx and dcruzo@ipn.mx

[2]Medical Robotics and Biosignals Lab, CIDETEC-Instituto Politécnico Nacional, Gustavo A. Madero, Mexico City. email: mgomezc2103@alumno.ipn.mx and mballesterose@ipn.mx

[3]Information Technology Department, Universidad de Medellín, Medellín, Colombia, email: magonzalez@udemedellin.edu.co

[4]Telecommunications Department, Engineering Faculty, Universidad de Antioquia, Medellín, Colombia email: diana.tobon@udea.edu.co

Gait is a highly complex process involving multiple systems and variables, making its analysis multifactorial. This comprehensive approach allows for a better understanding of the phenomenon by examining different aspects of body movement [4]. Traditionally, gait analysis is divided into three main approaches:

- Kinematic analysis: Focuses on the movement of body segments in space, evaluating spatiotemporal parameters like angles, displacement, velocity, and acceleration, without considering the forces causing the motion. Systems like Motion Capture (MoCap) and inertial sensor-based devices are used to collect these signals [5].
- Kinetic analysis: Examines the internal and external forces acting on body segments that generate movement. Tools such as force plates and pressure insoles provide data on ground reaction forces [6].
- Bioelectric analysis: Records the biopotentials generated by muscle contractions, typically assessed via surface electromyography (sEMG) [7].

Specifically, MoCap technology is widely used as a gold standard in kinematic gait analysis due to its high fidelity. Using high-speed infrared cameras and reflective markers placed on strategic anatomical points, MoCap systems record three-dimensional body movements. However, these systems are complex, costly, and require specialized operators [8], limiting their accessibility to well-equipped laboratories [9].

An alternative approach employs inertial measurement units (IMUs), which include accelerometers, gyroscopes, and magnetometers, to capture inertial signals from human locomotion [10]. Compared to MoCap, IMUs offer portability, lower cost, minimal maintenance, and usability in uncontrolled, real-world environments [11, 12]. Recent years have seen significant growth in IMU-based gait analysis systems, which are broadly categorized into three areas:

- Implementation of Euler angles (roll, pitch, and yaw) or quaternions to compute lower limb joint angles [10].
- Double integration of acceleration to estimate position and determine spatiotemporal gait parameters [13].
- Application of machine learning models to IMU data, such as acceleration and angular velocity, to estimate spatiotemporal parameters or detect pathologies [14].

However, previous IMU-based systems have reported limitations. For example, Bluetooth Low Energy communication protocols have exhibited latency and data instability issues, as demonstrated in [15], which showed significant throughput degradation under Wi-Fi interference, adversely affecting synchronization and data integrity. Additionally,

noise reduction filters often fail to adequately correct IMU drift [16], compromising kinematic accuracy.

In light of these challenges, the present study describes the development of an IMU-based system called STEPIO, which comprises four wireless modules and a user interface for data acquisition, visualization, processing, and storage. STEPIO addresses earlier limitations by implementing a transmission control protocol (TCP/IP) based wireless communication protocol and by integrating a complementary filter that fuses accelerometer-derived inclinations and gyroscope integrations to effectively compensate for long-term sensor drift, resulting in improved accuracy in gait parameter measurements. The system was tested on fifteen subjects and compared with results from a vision-based system.

II. System Description

Considering the limitations associated with MoCap systems, the STEPIO system has been developed for kinematic analysis of human gait without the need for complex facilities or a limited room. STEPIO is based on IMUs and Internet of Things (IoT) technology. This system enables the acquisition, processing, visualization, and storage of lower limb joint movement data, focusing on the hip and knee joints. The system has two elemental subsystems: one is the wireless portable modules, and the second is the software, which is a user interface based on Python. Figure 1 shows a diagram representing the STEPIO systems with these two elements.

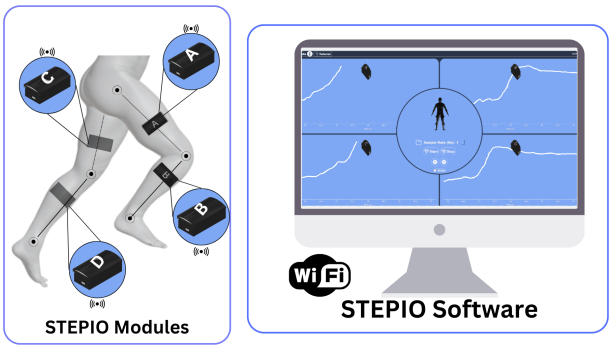

Fig. 1. STEPIO system, on the left side the four designed modules, on the right side the software developed for signals processing and visualization.

A. STEPIO Modules

This part of the system comprises four modules. Each module has a cover designed in Inventor® and manufactured using 3D printing. Each casing measures 85 mm × 40 mm × 25 mm in height, with each module identified by a letter (A to D) on the top (see Figure 2-i). Each module collects inertial gait data using an IMU of 6-axis LSM6DSOX and a 3-axis magnetometer LIS3MDL, which together provide 9 degrees of freedom (DoF) (see Figure 2-iv). The IMUs capture real-time acceleration, angular velocity, and orientation data across three axes (x, y and z). A 3.7 V Li-Po battery serves as the power source (see Figure 2-iii). The embedded system used an ESP-32 FireBeetle microcontroller, programmed in MicroPython via the Thonny IDE (see Figure 2-ii).

The physical system is illustrated in Figure 2, showing the placement of each component: i) case, ii) microcontroller, iii) power source, and iv) IMU sensor.

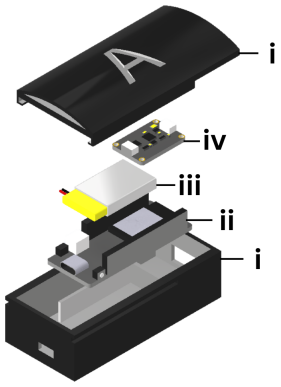

Fig. 2. STEPIO module elements.

The microcontroller collects and sends the signals as data frames to the master system using a TCP/IP socket-based communication at a sample rate of 100 Hz. For data acquisition, the gyroscope range is set to ±2000 deg/s (±34.90 rad/s), the accelerometer to ±8 g (±78.48 m/s^2), and the magnetometer to ±4 G (±400 µT). The units and variables for the collected data are:

- Magnetometer: Values are read along the three axes as mag_x, mag_y and mag_z in microteslas (µT).
- Accelerometer: Readings are obtained along the three axes as acc_x, acc_y and acc_z in meters per second squared (m/s²), then converted to g units.
- Gyroscope: Values are read along the three axes as gyr_x, gyr_y and gyr_z in radians per second (rad/s).

Additionally, the elapsed time since the start of the test, labeled $time$, is recorded. These data points are organized into a FRAME using the "@" as a terminator, as follows:

$$\textbf{FRAME} = \{mag_x, mag_y, mag_z, acc_x, acc_y, acc_z, gyr_x, gyr_y, gyr_z, time@\}.$$

B. Software Description

The STEPIO software features an intuitive GUI to facilitate user interaction with the system. It is structured into two main stages:

1) Connection Stage: The connection between the master system and the embedded system is established using TCP/IP sockets over a Wi-Fi network generated by the master system. Each microcontroller in the modules contains a `.json` file with network settings (Service Set Identifier (SSID), password, port, and the internet protocol (IP)), enabling it to connect to the network and create a socket for transmitting the collected FRAME (see Figure 3). The system connects to the local network on the designated port for each module and receives the transmitted FRAME. This process is executed in parallel by assigning a thread to each port.

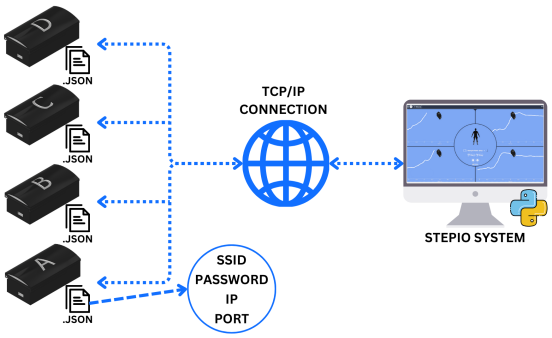

Fig. 3. General wireless connection diagram.

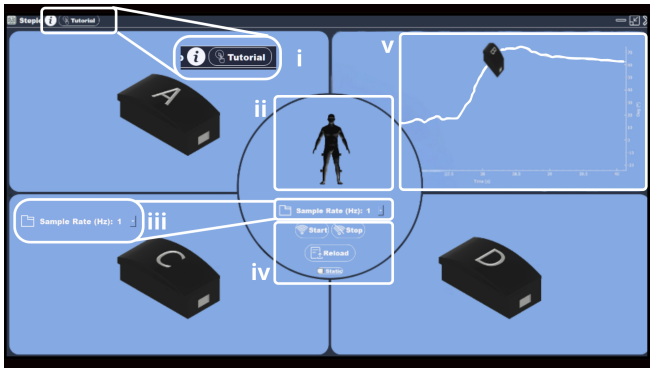

Fig. 4. Graphical user interface.

2) Acquisition Stage: A GUI was developed in Python using QtDesigner for data acquisition and interpretation. The GUI allows users to perform various tasks, such as viewing a tutorial for precise module placement, reviewing previously collected tests, and visualizing calculated angular signals. The interface is divided into five main stages: i) New User Assistance, ii) Status Window, iii) Communication, iv) Reload Previous Tests, and v) Signal Plotting.

- New User Assistance: It includes two buttons. The "Help" button provides access to the installation, user, and technical manuals, offering essential information. The second button plays a video tutorial of module placement as a guide for proper anatomical positioning (see Figure 4-i).
- Status Window: It displays a 3D figure of a person with the system integrated, providing a quick reference for module installation. Additionally, it shows an icon indicating the system status (e.g., connection, calibration, or video tutorial playback) (see Figure 4-ii).
- Communication Stage: It involves two steps. First, the user selects the storage location for the `.csv` files generated at the end of the test (see Figure 4-iii). A folder named after the test is created within this path, containing separate `.csv` files for each module with inertial signals and the corresponding joint angles. The file path follows the format: `C:\{file name}\{file name}_{module id}.csv`, once data transmission is terminated by pressing the "Stop" button.
- Reload Previous Tests: this block allows users to select a folder containing .csv files from a previous test and load it into the system for data visualization. Additionally, it provides scrollable x-axis functionality through two pop-up buttons (see Figure 4-iv).
- Signal Plotting: Finally, the plotting block offers online visualization of the approximate joint angle, calculated using Euler angles [17]. Specifically, the pitch angle is used, as it determines the module's inclination (upward or downward), as shown in Figure 4-v.

III. Data Online Processing

In (1), the computation of the inclination is described. This expression is used for each module and is based on the accelerometer data. Before performing this calculation, a Butterworth band-pass filter with a central frequency of 15 Hz is applied to reduce noise in the IMU signals generated by small mechanical vibrations and unexpected motion artifacts, reducing cumulative drift and preserving the relevant human motion information. From this initial calculation, the values obtained during the calibration phase, which consisted of averaging the tilt over the first 10 seconds, are averaged to determine an offset value. This value, denoted as θ_{offset}, is subtracted from subsequent readings to obtain the joint angle value.

$$\theta = \arctan\left(\frac{-acc_x}{\sqrt{acc_y^2 + acc_z^2}}\right) - \theta_{\text{offset}} \tag{1}$$

Subsequently, a complementary filter is applied to combine sensor measurements for a more accurate orientation estimation [16]. This filter fuses the angle θ calculated from accelerometer readings with gyroscope data to compensate for accelerometer drift caused by vibrations or linear accelerations. This is defined in (2).

$$\theta_{\text{estimate}} = \alpha\left(\theta_{\text{previous}} + gyr_y \Delta t\right) + (1-\alpha)\theta_{\text{raw}} \tag{2}$$

where:

- θ_{estimate} represents the filtered angle expressed in deg (the current orientation estimate).
- θ_{previous} is the estimated angle expressed in degrees from the previous step.
- gyr_y corresponds to the gyroscope reading on the y axis.
- Δt is the time interval between measurements, expressed in seconds.
- θ_{raw} is the unfiltered joint angle in degrees obtained from the accelerometer.
- α is the weighting factor, set to $\alpha = 0.01$. This value was fine-tuned via experimentation.

For the modules associated with the hip joint, θ_{estimate} is directly interpreted as the joint angle. However, for the knee joint, an adjustment is required, as shown in (3).

$$\theta_{\text{knee}} = \theta_{\text{hip}} - \theta_{\text{estimate}} \tag{3}$$

where θ_{estimate} corresponds to the angle calculated using (2) for the module assigned to the knee joint, and θ_{hip} represents the joint angle measured at the hip.

IV. Experimental Protocol

A. Participants

This study involved 15 adult participants (eight males and seven females, with a mean height of 1.76 ± 0.20 m, body mass of 84.5 ± 22.5 kg, and age of 20 ± 2 years). The experiments were conducted at the Medical Robotics and Biosignals Laboratory, UPIBI-IPN. The protocol was approved by Secretería de Investigación y Posgrado - IPN (SIP-20250223 and SIP-20250253), ensuring compliance with national ethical regulations and the Declaration of Helsinki.

Participants were chosen according to established inclusion and exclusion criteria without self-reported diagnosis of neuromusculoskeletal pathology. Demographic details, including occupation and lifestyle factors such as physical activity frequency, were also gathered from each individual.

B. Experimental Setup

The protocol incorporates an optical system and the STEPIO system for subsequent comparison.

1) Optical System: The system employs retroreflective markers composed of white LEDs powered by a 3 V lithium coin cell battery, encased in 3D-printed PLA cases with tabs for secure attachment using micropore tape. Following Winter's methodology [18], markers were positioned at key anatomical landmarks of the lower limb: the lower third of the lateral thigh surface (AS), the flexion-extension axis of the knee (TH-L), the upper third of the shank surface (TI-U) and the lateral malleolus along the transmalleolar axis (TI-L), as depicted in Figure 5.

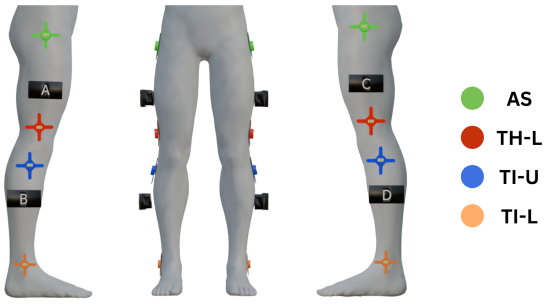

Fig. 5. Placement of retroreflective markers and STEPIO modules at anatomical points to obtain segments and angles of movement of the lower limb.

The markers facilitate the creation of segments for calculating lower limb movement angles, with motion data extracted from video recordings using MATLAB® software.

2) STEPIO system: As seen in Figure 5, each of the modules is placed according to the letter assigned on each housing, where the letter **A** is placed on the medial-lateral side of the right thigh, **B** on the medial-lateral side of the right leg, **C** on the medial-lateral side of the left thigh, and **D** on the medial-lateral side of the right leg.

C. Motion protocol

The motion protocol consists of two stages: Motion Tests and Gait.

1) Motion Test: : As illustrated in Figure 6, various positions are alternated, such as standing, sitting, knee bending, and knee lifting. Each of these movements is repeated five times, with an interval of approximately 30 seconds for rest between each test. A 10-second window is established to calibrate the STEPIO system properly.

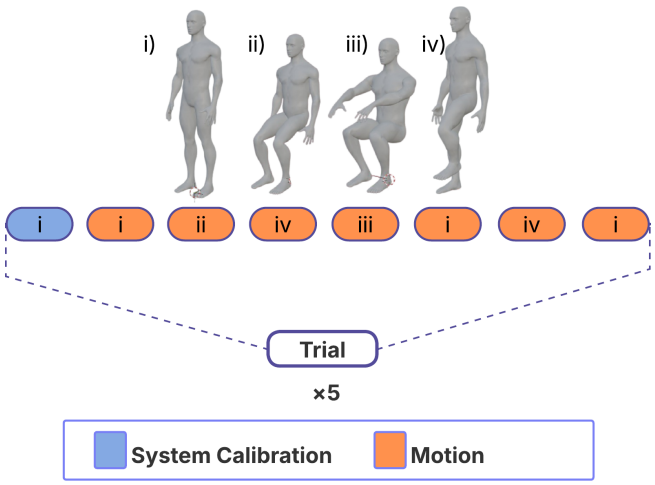

Fig. 6. Lower limb movement assessment protocol. i) Standing position. ii) Sitting position. iii) Knee flexion. iv) Right knee lift.

2) Gait: The gait stage consists of acquiring joint angles using videography and the STEPIO system during three walking sessions at speeds of 1 mph (0.447 m/s), 2 mph (0.894 m/s), and 3 mph (1.341 m/s) on an electric treadmill for 2 minutes. Each system independently estimates the angles of movement generated by each participant's lower limb to obtain the error percentages between the STEPIO and optical system.

V. Data Collection

Seven main folders were structured to create the dataset, each corresponding to a participant. Within each folder, the data were divided into two groups based on the system used:

A. Optical System (Reference)

1) Raw Data: Contains the binarized video generated during the test and a comma-separated values (CSV) file with frame number, inter-frame time intervals, start time, and end time.

2) Processed Data: Includes CSV files with time and joint angles homogenized at 100 samples per second.

B. STEPIO System

1) Raw Data: Stores a CSV file generated by the system, containing elapsed time, raw inertial signals, and estimated joint angles.

2) Processed Data: Contains CSV files with time and joint angles homogenized at 100 samples per second.

Additionally, each main folder was subdivided by test type to facilitate data organization and analysis. The dataset structure is illustrated in Figure 7.

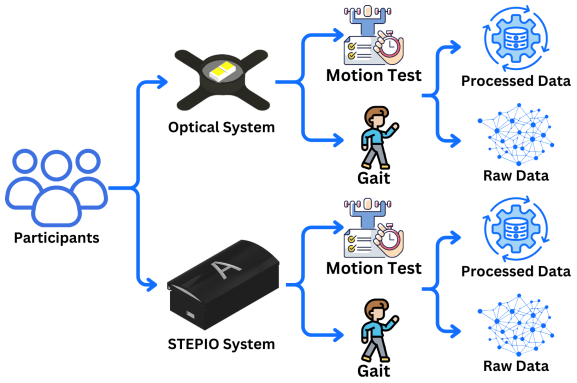

Fig. 7. Dataset structure.

C. Data Processing

The processing for the optical system consisted of:

- Binarization of video frames by adjusting exposure and contrast parameters to detect retroreflective markers accurately.
- Processing the raw CSV file generated during the test, which records the local time associated with each joint angle sample (hip and knee).

The raw CSV file from the STEPIO system contains, for each sample, the elapsed time since the test start, local timestamp, raw inertial sensor values (three axes), and the estimated joint angle. To homogenize and compare both datasets, the following steps were applied:

- Interpolation of optical and inertial data at 100 samples per second for further processing.
- Synchronization using local timestamps.
- Calculate the average joint angle from the optical system's first three seconds. This value served as an offset to adjust the signal to its baseline, removing bias caused by marker placement errors.

Processed and synchronized data were stored in the "Processed Data" folders of the dataset.

VI. Experimental Results

Three communication tests were conducted with all four modules connected simultaneously for five minutes to validate the wireless communication employed in the system (TCP/IP) and assess data loss. Subsequently, the sampling frequency was calculated based on the interval between successive samples, yielding an average frequency of 99.4 Hz and an average data loss of 0.58% on public networks, as shown in Table I.

To validate motion capture, a test was performed using the routine described in Figure 6, comparing the results obtained with those from the optical reference system, as shown in Figure 8. The results exhibited values similar to those of the

TABLE I
DATA LOSS TEST WITH AN EXPECTED FREQUENCY OF 100 HZ.

	Module A	Module B	Module C	Module D
Test 1	99.4 Hz	99.4 Hz	99.4 Hz	99.4 Hz
Test 2	99.4 Hz	99.3 Hz	99.4 Hz	99.4 Hz
Test 3	99.4 Hz	99.4 Hz	99.5 Hz	99.5 Hz
Packet Loss	0.6%	0.63%	0.56%	0.56%

reference system, with a root mean squared error (RMSE) of 2.7 deg and a standard deviation (SD) of 2.44 deg, thereby confirming the precision of the STEPIO system.

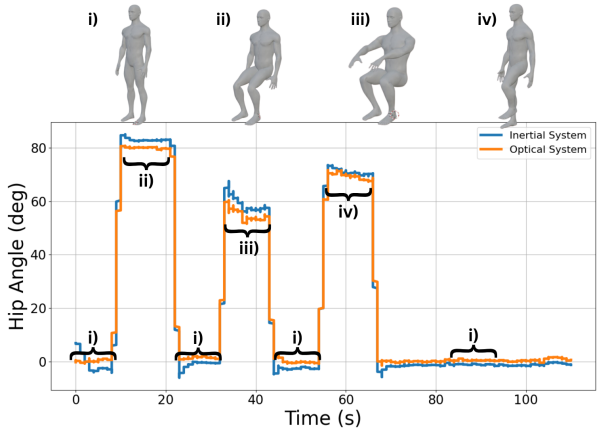

Fig. 8. Processed signal comparison: optical system (blue) vs. STEPIO (orange).

Regarding human gait analysis, three treadmill speeds (0.447 m/s, 0.894 m/s and 1.341 m/s) were evaluated, by identifying every gait cycle on all participants and three different speeds. After segmentation and normalization of those cycles, the average graph was computed, illustrated in Figure 9. Furthermore, the SD of 1.732 deg for the hip and 4.956 deg for the knee confirmed the replicability of the gait cycle measurements.

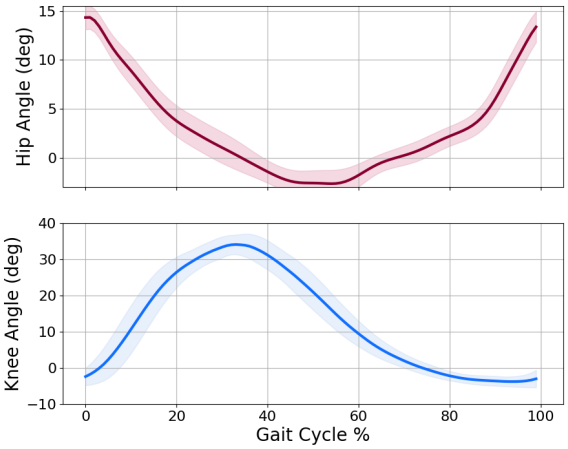

Fig. 9. Comparison of hip and knee gait cycles recorded at a speed of 1 mph (1.6 km/h).

Finally, a simulation was performed using CoppeliaSim®, in which the vectors stored in the dataset obtained during the movement test described in the experimental protocol were introduced. The simulation outcome shows the relationship between the actual physical movement and the movement represented by the data collected by the STEPIO system, deploying the joint's anatomic movement, see Figure 10.

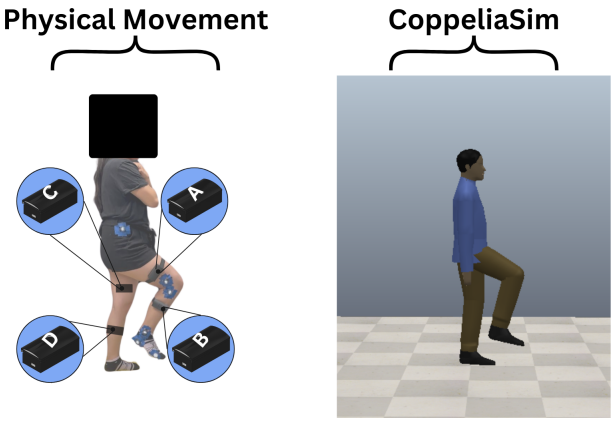

Fig. 10. Human locomotion simulation in CoppeliaSim®, showing STEPIO module placement and retroreflective marker positions.

VII. Conclusions

The STEPIO system has proven to be a robust and reliable tool for kinematic gait analysis in uncontrolled environments. Its modular design, online interface, and TCP/IP-based wireless communication by a stable average sampling frequency of 100 Hz enable accurate joint angle estimation with performance comparable to traditional optical systems. Also, quantitative results, including an RMSE value of 2.7 deg, a mean deviation of 2.4 deg compared to the reference optical system. In addition, an SD regarding segmented and normalized gait cycle angles of 1.732 deg and 4.956 deg for the hip and knee, respectively, proves the system's precision and data integrity. Overall, STEPIO offers a cost-effective, portable, and efficient alternative for clinical evaluations and biomechanical research.

References

[1] Michael W Whittle. *Gait analysis: an introduction*. Butterworth-Heinemann, 2014.

[2] Federico Roggio, Bruno Trovato, Martina Sortino, Michele Vecchio, and Giuseppe Musumeci. Self-selected speed provides more accurate human gait kinematics and spatiotemporal parameters than overground simulated speed on a treadmill: a cross-sectional study. *BMC Sports Science, Medicine and Rehabilitation*, 16(1):226, 2024.

[3] Zhennan Li, Yang Han, Chunbao Liu, Haohua Xiu, Guowu Wei, and Lei Ren. Design, manufacture, and experimental validation of a hydraulic semi-active knee prosthesis. *IEEE Transactions on Neural Systems and Rehabilitation Engineering*, 31:1394–1404, 2023.

[4] Rosie Morris, Aodhán Hickey, Silvia Del Din, Alan Godfrey, Sue Lord, and Lynn Rochester. A model of free-living gait: A factor analysis in parkinson's disease. *Gait & posture*, 52: 68–71, 2017.

[5] Weijun Tao, Tao Liu, Rencheng Zheng, and Hutian Feng. Gait analysis using wearable sensors. *Sensors*, 12(2):2255–2283, 2012.

[6] Mariana Alegria, Citlali Alvarado, Mariana Ballesteros, Diana Tobon-Vallejo, and David Cruz-Ortiz. Development of a wearable device for analyzing plantar load in the human gait cycle. In *2023 11th International Conference on Control, Mechatronics and Automation (ICCMA)*, pages 7–12. IEEE, 2023.

[7] Carlo Frigo and Paolo Crenna. Multichannel semg in clinical gait analysis: a review and state-of-the-art. *Clinical Biomechanics*, 24(3):236–245, 2009.

[8] Marcello Fusca, Francesco Negrini, Paolo Perego, Luciana Magoni, Franco Molteni, and Giuseppe Andreoni. Validation of a wearable imu system for gait analysis: Protocol and application to a new system. *Applied Sciences*, 8(7):1167, 2018.

[9] Dominic Thewlis, Chris Bishop, Nathan Daniell, and Gunther Paul. Next-generation low-cost motion capture systems can provide comparable spatial accuracy to high-end systems. *Journal of applied biomechanics*, 29(1):112–117, 2013.

[10] Udomporn Manupibul, Ratikanlaya Tanthuwapathom, Wimonrat Jarumethitanont, Panya Kaimuk, Weerawat Limroongreungrat, and Warakorn Charoensuk. Integration of force and imu sensors for developing low-cost portable gait measurement system in lower extremities. *Scientific Reports*, 13(1):10653, 2023.

[11] Cortney Armitano-Lago, Dominic Willoughby, and Adam W Kiefer. A swot analysis of portable and low-cost markerless motion capture systems to assess lower-limb musculoskeletal kinematics in sport. *Frontiers in Sports and Active Living*, 3: 809898, 2022.

[12] Anita Sant'Anna, Nicholas Wickström, Helene Eklund, Roland Zügner, and Roy Tranberg. Assessment of gait symmetry and gait normality using inertial sensors: in-lab and in-situ evaluation. In *Biomedical Engineering Systems and Technologies: 5th International Joint Conference, BIOSTEC 2012, Vilamoura, Portugal, February 1-4, 2012, Revised Selected Papers 5*, pages 239–254. Springer, 2013.

[13] Alberto Ferrari, Pieter Ginis, Michael Hardegger, Filippo Casamassima, Laura Rocchi, and Lorenzo Chiari. A mobile kalman-filter based solution for the real-time estimation of spatio-temporal gait parameters. *IEEE transactions on neural systems and rehabilitation engineering*, 24(7):764–773, 2015.

[14] Dante Trabassi, Mariano Serrao, Tiwana Varrecchia, Alberto Ranavolo, Gianluca Coppola, Roberto De Icco, Cristina Tassorelli, and Stefano Filippo Castiglia. Machine learning approach to support the detection of parkinson's disease in imu-based gait analysis. *Sensors*, 22(10):3700, 2022.

[15] Bozheng Pang, Tim Claeys, Kristof T'Jonck, Hans Hallez, and Jeroen Boydens. Bluetooth low energy reliability and throughput under wi-fi interference. In *2022 XXXI International Scientific Conference Electronics (ET)*, pages 1–4. IEEE, 2022.

[16] Yu Guan and Xinmin Song. Sensor fusion of gyroscope and accelerometer for low-cost attitude determination system. In *2018 Chinese Automation Congress (CAC)*, pages 1068–1072. IEEE, 2018.

[17] James Diebel et al. Representing attitude: Euler angles, unit quaternions, and rotation vectors. *Matrix*, 58(15-16):1–35, 2006.

[18] D.A. Winter. *Biomechanics and Motor Control of Human Movement*. Wiley, 2009. ISBN 9780470398180. URL https://books.google.com.mx/books?id=_bFHL08IWfwC.